Stable-Isotope-Assisted NMR Studies on ^{13}C-Enriched Sialyl Lewis^x in Solution and Bound to E-Selectin

Richard Harris,[†] Graham R. Kiddle,[†] Robert A. Field,[†] Mark J. Milton[⊥,†], Beat Ernst,[‡,||] John L. Magnani,[§] and Steve W. Homans*[,†]

Contribution from the Centre for Biomolecular Sciences, University of St. Andrews, St. Andrews, KY16 9ST U.K., Novartis Pharma AG, CH-4002 Basel, Switzerland, and GlycoTech Corporation, Rockville, Maryland 20850

Received September 25, 1998. Revised Manuscript Received January 15, 1999

Abstract: We report the determination of the solution structure and dynamics of ^{13}C-enriched Neu5Acα2−3Galβ1−4(Fucα1−3)GlcNAc (sialyl Lewis^x), together with its bound-state conformation in association with E-selectin. The availability of ^{13}C-enriched material enabled both the measurement of trans-glycosidic ^{13}C−^{13}C coupling constants as conformational probes in the tetrasaccharide and the application of three-dimensional nuclear Overhauser effect ^{13}C−^{1}H heteronuclear single-quantum correlation experiments for the measurement of intramolecular transferred nuclear Overhauser effects (TRNOEs) characterizing the bound-state conformation of the ligand. The additional dispersion afforded by the third (^{13}C) dimension permitted straightforward identification and quantitation of these TRNOEs, and several TRNOEs were identified that had not previously been reported. The bound-state conformation of the ligand, determined by use of a heteronuclear full-relaxation matrix analysis of the TRNOE data, differs significantly from that reported in previous studies.

Introduction

The role of the tetrasaccharide sialyl Lewis^x (sLe^x, Neu5Acα2−3Galβ1−4(Fucα1−3)GlcNAc) as a ligand for the selectin family of receptors in the adhesion of leukocytes and neutrophils to vascular endothelial cells during inflammatory responses has been well documented.[1] A complete understanding of the molecular basis of recognition of sLe^x by the selectins ideally requires high-resolution structural data for the complex. Since such data are not available to date, studies have focused on the bound-state conformation of the ligand determined by use of transferred nuclear Overhauser effect (TRNOE) measurements. Four studies have appeared which report different bound-state conformations for the ligand.[1−5] A major difficulty with such studies is the severe resonance overlap of proton resonances in the ligand, which renders difficult the identification of all available intraligand TRNOEs and severely compromises the measurement of TRNOE intensities. To overcome these difficulties, we report here the application of heteronuclear three-dimensional NMR methods[6] for the measurement of TRNOEs in ^{13}C-enriched sLe^x[7] bound to E-selectin. The additional spectral dispersion afforded by the third (^{13}C) dimension enables the determination of TRNOE intensities with good accuracy; moreover, several TRNOEs are observed that have not been reported previously. In addition, we reinvestigate the solution structure and dynamics of the free tetrasaccharide with inclusion of transglycosidic ^{13}C−^{13}C coupling constant measurements and Overhauser effects involving exchangeable protons.

Materials and Methods

Sample Preparation. (i) Free Solution Studies. Five milligrams of Neu5Acα2−3Galβ1−4[Fucα1−3]GlcNAc (Dextra) and 2 mg of *N*-acetyl [^{13}C]Neu5Acα2−3Galβ1−4[Fucα1−3]GlcNAc[7] were dissolved and lyophilized into 99.96% D_2O three times, followed by dissolution into 750 mL of D_2O. For the observation of the exchangeable protons, the natural abundance Neu5Acα2−3Galβ1−4[Fucα1−3]-GlcNAc was dissolved in 750 mL of H_2O containing 15% 99.96% acetone-d_6 (Cambridge Isotopes). The pH was adjusted to between 5.5 and 6.0 by careful stepwise addition of dilute HCl or NaOH and transferred to a 5-mm NMR tube. The sample was degassed by sonication for about 1 min.

(ii) Bound Conformation Studies. The E-selectin utilized in this study is a recombinant chimera of E-selectin and human IgG, in which the lectin, the EGF, and six CR domains of the E-selectin replace the antigen binding sites in IgG. This material was prepared as described.[3] For NMR analysis, 10 mg of the chimera was dialyzed against 50 mM [D_4]imidazole buffer containing 1 mM $CaCl_2$, in D_2O, pD 7.4. The sample was concentrated by use of a Centricon concentrator (YM-50, Amicon) to a final volume of 600 μL, and ^{13}C-enriched sLe^x was added to a concentration 15-fold greater than the concentration of E-selectin binding sites in the chimera.

NMR Experiments. (i) Free Solution Studies. NMR spectra were obtained at 303 and 258 K with a reference frequency of 500 MHz on a Varian Unityplus spectrometer equipped with a self-shielded *z* gradient

* To whom correspondence should be addressed.
[†] University of St. Andrews.
[‡] Novartis Pharma AG.
[§] GlycoTech Corp.
[⊥] Present address: Department of Chemistry, University of Alberta, Edmonton, Alberta, Canada.
[||] Present address: Department of Pharmacy, University of Basel, CH-4051 Basel, Switzerland.

(1) Hensley, P.; McDevitt, P. J.; Brooks, I.; Trill, J. J.; Feild, J. A.; McNulty, D. E.; Connor, J. R.; Griswold, D. E.; Kumar, N. V.; Kopple, K. D.; Carr, S. A.; Dalton, B. J.; Johanson, K. J. *J. Biol. Chem.* **1994**, *269*, 23949−23958.
(2) Cooke, R. M.; Hale, R. S.; Lister, S. G.; Shah, G.; Weir, M. P. *Biochemistry* **1994**, *33*, 10591−10596.
(3) Scheffler, K.; Ernst, B.; Katopodis, A.; Magnani, J. L.; Wang, W. T.; Weisemann, R.; Peters, T. *Angew. Chem., Int. Ed. Engl.* **1995**, *34*, 1841−1844.
(4) Scheffler, K.; Brisson, J.-R.; Weisemann, R.; Magnani, J. L.; Wong, W. T.; Ernst, B.; Peters, T. *J. Biomol. NMR* **1997**, *9*, 423−436.
(5) Poppe, L.; Brown, G. S.; Philo, J. S.; Nikrad, P. V.; Shah, B. H. *J. Am. Chem. Soc.* **1997**, *119*, 1727−1736.
(6) Kay, L. E.; Marion, D.; Bax, A. *J. Magn. Reson.* **1989**, *84*, 72−84.
(7) Probert, M. A.; Milton, M. J.; Harris, R.; Schenkman, S.; Brown, J. M.; Homans, S. W.; Field, R. A. *Tetrahedron Lett.* **1997**, *38*, 5861−5864.

10.1021/ja983423y CCC: $18.00
Published on Web 03/05/1999

triple-resonance probe. Two-dimensional (2D) heteronuclear single-quantum correlation (HSQC) experiments were recorded with a total of 512 complex and 2K complex points in the t_1 and t_2 dimensions, respectively, with spectral widths of 9.3 and 2 kHz. Four scans were acquired per t_1 increment, with a total acquisition of 3 h. Two-dimensional HCCH correlated spectroscopy (COSY) experiments were recorded using the three-dimensional (3D) pulse scheme described.[8,9] A total of 256 complex and 2K complex points were acquired in the t_1 and t_2 dimensions, respectively, with spectral widths of 9.3 and 2 kHz. Two- and three-dimensional gradient-enhanced long-range carbon−carbon *J*-correlation (LRCC) experiments[10,11] were recorded with a proton spectral width of 2.1 kHz, consisting of 1K complex points, and a ^{13}C spectral width of 9.6 kHz in t_1 (256 complex points) and 9.6 kHz (32 complex points) in t_2 for the 3D experiment. ^{13}C−^{13}C couplings evolve and are refocused during the delay (4 T) of 44.4 ms. Totals of 64 and 8 scans were acquired per increment for the 2D and 3D experiments with total acquisition times of ∼24 and ∼48 h, respectively. The values of the long-range coupling constants are derived from the ratios of the cross-peak volumes obtained in the spectrum in the manner described.[11]

Three-dimensional rotating frame Overhauser effect spectroscpoy (ROESY)−HSQC experiments were acquired with offset compensation[12] and with spectral widths of 1.9, 7, and 1.9 kHz and 128, 32, and 1024 complex points in t_1, t_2, and t_3, respectively. The proton offset was placed 200 Hz upfield of the highest field resonance during the spin-lock period to minimize coherence effects. To optimize digital resolution, the GlcNAc C-8 and Neu5Ac C-3 resonances were folded-in once, with the incremental delay at time zero in t_2 calculated to give a processed spectrum in which the folded peaks have a phase opposite to that of nonfolded peaks when zero- and first-order phases are set to 90° and −180°, respectively. The effective field for spin-locking was 2 kHz and was applied for 100 ms. Prior to Fourier transformation, data were apodized with cosine-bell functions, and the t_1 and t_2 dimensions were zero-filled to 256 and 64 complex points, respectively. The total acquisition time for the 3D experiment was ∼55 h.

Two-dimensional COSY, nuclear Overhauser effect spectroscopy (NOESY), and ROESY experiments incorporating excitation sculpting (ES) water suppression[13] were acquired at 258 K with spectral widths of 3.8 kHz, 512 t_1 increments, 32 scans per increment, and 4K complex points in t_2. The length of the mixing times in the (ES)NOESY and (ES)ROESY experiments was 100 ms. Prior to 2D Fourier transformation, data were apodized using cosine-bell functions. Hydroxyl exchange rates were measured using the method described by Adams and Lerner[14] incorporating excitation sculpting water suppression.[13] Spectra were acquired with 16 scans, 4K complex points, and a spectral width of 3.8 kHz and were recorded with saturation times varying from 0 to 1 s. ES-1D ^{1}H spectra were acquired with a proton spectral width of 4 kHz and 8K points.

Bound-State Conformational Studies. Three-dimensional NOESY−HSQC experiments were recorded at 500 MHz with a Varian Unityplus spectrometer using a sample prepared as above. The probe temperature was 300 K in all experiments. A total of 128 × 32 × 512 complex points were acquired in the t_1,t_2,t_3 dimensions of the 3D spectrum, with proton (*F*1,*F*3) spectral widths of 2130 Hz and a carbon (*F*2) spectral width of 7000 Hz. The mixing time (τ_m) was 150 ms. Prior to 3D Fourier transformation, time domain data were apodized with cosine-bell weighting functions in each dimension.

TRNOE Simulations. Experimental TRNOE intensities were measured directly as volume integrals from 2D *F*1/*F*3 planes derived from 3D NOESY−HSQC spectra, and integrals were summed for each plane that contained a contribution from the relevant cross-peak to give the 3D volume integral. Transferred NOE simulations were computed with the in-house-written software package MDNOE2. This package incorporates a full-relaxation matrix analysis of TRNOEs[15] and includes a formalism for computation of the relaxation matrix which accounts for internal motions which are fast with respect to the rotational tumbling time.[16] Simulations utilized the following parameters: rotational correlation time of the ligand (τ_{cL}) = 0.24 ns; rotational correlation time of the complex (τ_{cR}) = 110 ns; reduced rate constant (k) = 177 s^{-1} (corresponding to the literature value[5] of k_{off} = 164 s^{-1}); dissociation constant (K_d) = 0.72 mM;[5] concentration of E-selectin binding sites in the chimera ([R]) = 114 μM; concentration of ^{13}C-sLe^x ([L]) = 1.7 mM; mixing time (τ_m) = 0.15 s.

Molecular Modeling. All dynamics simulations were performed in vacuo with a dielectric constant (ϵ) of 80.0 and at a temperature of 300 K for simulations describing the dynamics of the free oligosaccharide. The AMBER force field[17] with a carbohydrate parameter set developed by Homans[18] was used with the exo-anomeric potentials set to zero. Simulations using time-averaged restraints were performed with XPLOR,[19] where an initial 50 ps of "conventional" restrained dynamics was used to equilibrate the system, and then 1-ns time-averaged restrained trajectories were performed. NOE/ROE distance restraints were classified as "weak", "medium", or "strong" and were applied as biharmonic restraints with lower and upper bounds of 1.8−2.7 (strong), 1.8−3.3 (medium), and 1.8−5.0 Å (weak), with a "memory time" τ = 50 ps.

Definitions of Dihedral Angles. The torsion angles ϕ and ψ are defined as H-1−C-1−O-1−C-X (C-1−C-2−O-2−C-X in the case of Neu5Ac) and C-1−O-1−C-X−H-X (C-2−O-2−C-X−H-X in the case of Neu5Ac), respectively, where C-X and H-X are aglyconic atoms.

Results and Discussion

Spectral Assignments. Complete ^{13}C and nonexchangeable ^{1}H resonance assignments for uniformly ^{13}C-enriched sLe^x were obtained from 2D ^{1}H−^{13}C HCCH−COSY and 2D ^{1}H−^{13}C HSQC experiments (not shown) and are essentially in agreement with previous work.[20] Exchangeable ^{1}H resonance assignments were obtained from 2D ES ^{1}H−^{1}H COSY and total correlation spectroscopy (TOCSY) experiments and are in good agreement with previously reported values for sLe^x in supercooled water.[5]

Solution Structure and Dynamics of the Free Tetrasaccharide. Previous studies on the structure and dynamics of sLe^x relied primarily on 2D ^{1}H−^{1}H Overhauser effect measurements. However, the analysis of such spectra is not straightforward because of the severe overlap in the ^{1}H dimension. In contrast, the assignment of ROEs from a 3D ROESY−HSQC spectrum is relatively straightforward because the cross-peaks are dispersed by their ^{13}C chemical shifts. Representative *F*2/*F*3 planes from the 3D spectrum at the *F*1 resonance frequencies of Gal H-1 (a) and Gal H-3 (b) are shown in Figure 1. From these spectra, four inter-glycosidic ROEs are observed, including ROEs from Gal H-3 to both Neu5Ac H-3ax and Neu5Ac H-8. These data alone confirm the flexibility of the Neu5Acα2−3Gal linkage in solution, since both ROEs cannot exist simultaneously for a given, fixed conformation. Similarly, a further five inter-glycosidic NOEs between Fuc and GlcNAc, and between Fuc and Gal residues, could be assigned in other *F*2/*F*3 planes (data not shown). In contrast to the NOEs observed

(8) Bax, A.; Clore, G. M.; Driscoll, P. C.; Gronenborn, A. M.; Ikura, M.; Kay, L. E. *J. Magn. Reson.* **1990**, *87*, 620−627.
(9) Yu, L.; Goldman, R.; Sullivan, P.; Walker, G. F.; Fesik, S. W. *J. Biomol. NMR* **1993**, *3*, 429−441.
(10) Bax, A.; Delaglio, F.; Grzesiek, S.; Vuister, G. W. *J. Biomol. NMR* **1994**, *4*, 787−797.
(11) Bax, A.; Max, D.; Zax, D. *J. Am. Chem. Soc.* **1992**, *114*, 6923−6925.
(12) Griesinger, C.; Ernst, R. R. *J. Magn. Reson.* **1987**, *75*, 261−271.
(13) Hwang, T. L.; Shaka, A. J. *J. Magn. Reson.* **1995**, *A112*, 275−279.
(14) Adams, B.; Lerner, L. *J. Magn. Reson.* **1992**, *96*, 604−607.
(15) London, R. E.; Perlman, M. E.; Davis, D. G. *J. Magn. Reson.* **1992**, *97*, 79−98.
(16) Tropp, J. *J. Chem. Phys.* **1980**, *72*, 6035−6044.
(17) Weiner, S. J.; Kollman, P. A.; Nguyen, D. T.; Case, D. A. *J. Comput. Chem.* **1986**, *7*, 230−252.
(18) Homans, S. W. *Biochemistry* **1990**, *29*, 9110−9118.
(19) Brünger, A. T. *X-PLOR−A System for X-ray Crystallography and NMR*; Yale University Press: New Haven, CT, 1987.
(20) Ichikawa, Y.; Lin, Y.-C.; Dumas, D. P.; Shen, G.-J.; Garcia-Junceda, E.; Williams, M. A.; Bayer, R.; Ketcham, C.; Walker, L. E.; Paulson, J. C.; Wong, C.-H. *J. Am. Chem. Soc.* **1992**, *114*, 9283−9298.

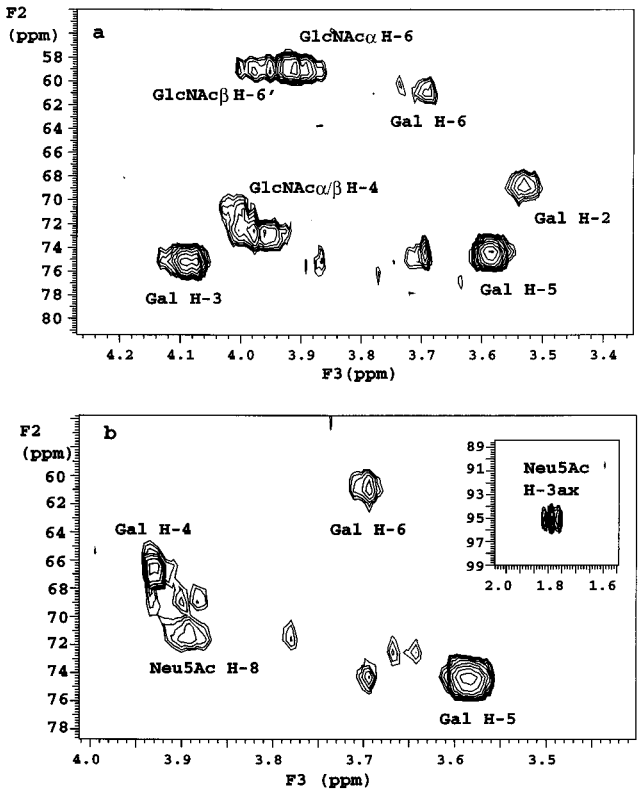

Figure 1. *F*2/*F*3 planes from the 3D ROESY−HSQC spectrum of ^{13}C-enriched sLe^x (τ_m = 100 ms), at the *F*1 resonance frequency of (a) Gal H-1 and (b) Gal H-3. Unlabeled cross-peaks correspond with crosstalk from adjacent planes.

for Neu5Acα2−3Galβ1−4Glc,[21] no evidence of the "anti" conformer was observed about the Galβ1−4GlcNAc linkage in sLe^x.

NOEs Involving Hydroxyl Protons. A number of inter-glycosidic NOEs are observable in the 2D ES-NOESY spectrum of sLe^x, pH ~6, at 258 K (not shown). Three inter-glycosidic NOEs about the Neu5Acα2−3Gal could be unambiguously identified between Gal OH-2−Neu5Ac H-3ax, Gal OH-4−Neu5Ac H-3eq, and Gal H-3−Neu5Ac OH-8, while a further NOE to Gal OH-2 (δ_H = 3.90) could not be assigned unambiguously but is probably a contribution of two NOEs, namely Gal OH-2−Neu5Ac H-8 and Gal OH-2−GlcNAc H-6's. In total, 10 inter-glycosidic NOEs involving exchangeable protons were observed which, in combination with NOEs between nonexchangeable protons, were utilized in further molecular modeling studies.

Time-Averaged Restrained Molecular Dynamics Simulations. In a previous study, we examined the solution dynamics of sLe^x by use of conventional restrained molecular dynamics simulations.[22] In the present study, the much larger number of available conformational restraints enables the application of time-averaged distance restraining protocols.[23] The advantage of the latter is that conformational transitions between regions of conformational space that are disconnected on the potential surface are not rendered inaccessible by the presence of the distance restraints, thus potentially giving a more realistic picture of the true dynamic properties of the molecule. The instantaneous values of ϕ vs ψ for each disaccharide linkage in sLe^x over the time course of a 1-ns in vacuo molecular dynamics simulation with time-averaged restraints are shown in Figure 2. To assess the validity of this simulation, time-averaged NOE (ROE) values were back-calculated from the simulation using a full-relaxation matrix approach, incorporating the solvent exchange rates for exchangeable protons listed in Table 1. The results of these calculations are compiled in Table 2. It is seen that most of the experimentally determined NOE (ROE) values are reproduced with good accuracy from the simulation. Notable exceptions are NOEs involving Gal OH-4. In particular, a substantial NOE between Gal OH-4 and Fuc H-3 is predicted in the simulation, whereas the experimental intensity of this NOE is extremely small. This can be rationalized in view of the fact that Gal OH-4 is proposed to be involved in a hydrogen bond to Neu5Ac COOH in solution,[5] which would tie this hydroxyl group away from the fucose residue and hence reduce the NOE to Fuc H-3. A repeat simulation with this proposed hydrogen bond incorporated as a distance restraint confirmed

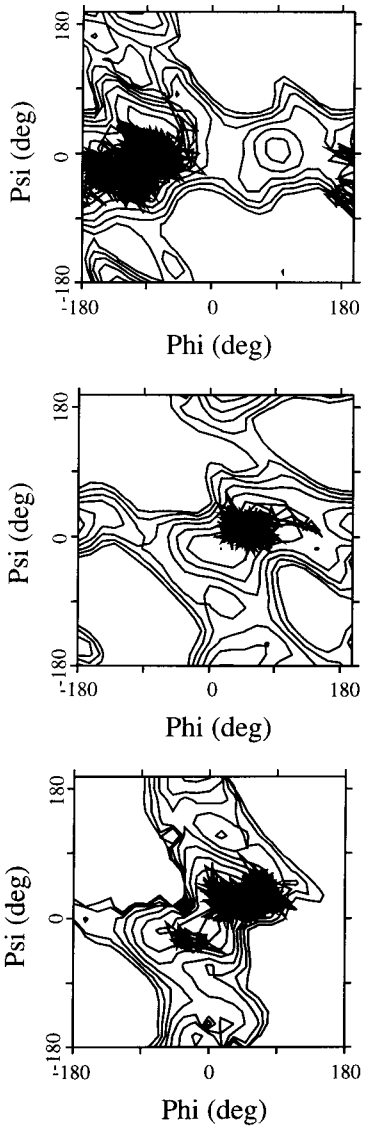

Figure 2. Intantaneous values of ϕ vs ψ during the time course of a 1-ns in vacuo simulation of sLe^x with time-averaged distance restraints. Panels correspond with (top) Neu5Acα2−3Gal, (center) Galβ1−4GlcNAc, and (bottom) Fucα1−3GlcNAc. Instantaneous values are superimposed on the potential surface of the relevant disaccharide contoured in 1 kcal/mol intervals to 6 kcal/mol.

(21) Milton, M. J.; Harris, R.; Probert, M.; Field, R. A.; Homans, S. W. *Glycobiology* **1998**, *8*, 147−153.
(22) Rutherford, T. J.; Spackman, D. G.; Simpson, P. J.; Homans, S. W. *Glycobiology* **1994**, *4*, 59−68.
(23) Torda, A. E.; Scheek, R. M.; van Gunsteren, W. F. *J. Mol. Biol.* **1990**, *214*, 223−235.

Table 1. NMR Data for the Exchangeable Protons from sLe^x in H_2O/Acetone-d_6 (85:15) at 258 K

proton	chemical shift (ppm)[a]	exchange rate (s^{-1})[b]
Neu5Ac OH-4	6.45	8.7 (21.2)
Neu5Ac OH-7	5.87	4.7 (19.1)
Neu5Ac OH-8	6.30	7.4 (13.5)
Neu5Ac OH-9	~5.87	nd[c]
Neu5Ac NH-5	8.31	
Gal OH-2	5.78	2.6 (6.3)
Gal OH-4	5.48	nd[c] (~5.5)
Gal OH-6	6.09	14.3 (40.2)
Fuc OH-2	nd[c]	nd[c]
Fuc OH-3	5.98	11.9 (31.8)
Fuc OH-4	5.91	11.0 (21.8)
GlcNAcα OH-1	7.23	7.6 (22.9)
GlcNAcα OH-6	5.95	13.1 (32.3)
GlcNAcα NH-2	8.57	
GlcNAcβ OH-1	7.87	10.3 (29.5)
GlcNAcβ OH-6	6.02	12.3 (34.2)
GlcNAcβ NH-2	8.63	

[a] Chemical shifts referenced to $\delta_{TSP} = 0.00$ ppm (by setting residual acetone to 2.19 ppm). [b] Exchange rates measured at 258 and 268 K (figures in parentheses). [c] Not determined.

Table 2. Back-Calculated Inter-Glycosidic NOEs and ROEs (Negative Values) Derived from a 1-ns in Vacuo Time-Averaged Restrained MD Simulation for sLe^x

NOE/ROE	theoretical[a]	experimental[a]
Fuc H-1−GlcNAc H-3	1.6	1.8
Fuc H-1−GlcNAc H-2	0.2	0.2
Gal H-1−GlcNAc H-4	1.4	0.8
Gal H-1−GlcNAc H-61	1.5	1.2
Gal H-2−Fuc H-5	1.3	0.9
Gal H-2−Fuc H-61	0.7	1.0
Gal H-61−Fuc H-3	0.9	1.0
Gal H-3−Neu5Ac H-3ax	0.4	0.6
Gal H-3−Neu5Ac H-8	0.3 (0.4)[b]	0.5
Gal H-1−GlcNAc OH-6	−0.5	−0.5
Gal OH-2−GlcNAc H-6	−0.6 (−0.4)	0.8[c]
Gal OH-2−Neu5Ac H-8	−0.2 (−0.3)	
Fuc H-1−GlcNAc NH	−1.3	−1.8
Gal OH-2−Fuc H-6	−0.1 (−0.1)	−0.1
Gal OH-4−Fuc H-6	−0.6 (−0.3)	−0.2
Gal OH-4−Fuc H-4	−0.4 (−0.2)	−0.3
Gal OH-4−Neu5Ac H-3eq	−0.0 (−0.1)	−0.1
Gal OH-2−Neu5Ac H-3ax	−0.4 (−0.3)	−0.9
Gal H-3−Neu5Ac HO-8	−0.1 (−0.3)	−0.5
Gal OH-4−Fuc H-3	−0.6 (−0.0)	nd[d]

[a] Values are relative NOEs and ROEs with respect to the intraresidue NOE/ROE between Gal H-1 and Gal H-3, which is defined as unit intensity. Theoretical values are time-averaged values computed from a full-relaxation matrix analysis ($\tau_m = 0.24$ ns). [b] Values in parentheses correspond with a simulation in which hydrogen-bond restraints have been included between Gal OH-4−Neu5Ac COOH and between Neu5Ac HO-8−Neu5Ac COOH. [c] Sum of values due to resonance overlap. [d] Not detected.

this hypothesis, with NOEs to Fuc H-4, H-6, and H-3 all agreeing with the experimental data (Table 2). In a similar manner, the Gal H-3−Neu5Ac H-8/HO-8 conflicting NOEs are only modeled well with an inclusion of the hydrogen bond Neu5Ac HO-8···Neu5Ac COOH. The proposed hydrogen bonds are consistent with the slower exchange rates listed in Table 1 for the relevant hydrogen bond donors and are consistent with previous observations.[24]

Trans-Glycosidic Coupling Constants. To validate further the dynamic properties of the tetrasaccharide predicted from molecular dynamics simulations, experimental trans-glycosidic heteronuclear $^1H-^{13}C$ and homonuclear $^{13}C-^{13}C$ coupling constants were compared with time-averaged values derived from the simulations using the appropriate Karplus parametrizations. The experimental values for the transglycosidic heteronuclear coupling constants have been described,[25] whereas the homonuclear coupling constants were measured by use of conventional 3D LRCC experiments[11] (data not shown). It is shown (Table 3) that theoretical values are, in general, in good agreement with experimental values, further validating the dynamic properties of the glycan derived from the molecular dynamics simulations. Overall, the dynamic properties of the glycan are similar to those proposed on the basis of conventional restrained dynamics simulations. However, all of the glycosidic linkages exhibit greater degrees of conformation freedom, a result that is anticipated in view of the much weaker instantaneous effective restraining force in simulations employing time-averaged restraints. Of particular interest is the fact that the Fucα1−3GlcNAc linkage appears to access an alternative conformation given by $\phi,\psi \approx -30°,-20°$ for a significant period of time. In addition, it is worthy of note that the theoretical ROEs between Gal H-3−Neu5Ac H-3ax and Gal H-3−Neu5Ac H-8 compare favorably with the experimental values, suggesting that the dynamic properties inferred from the simulation are a plausible model of the true solution behavior. Taken together, these data suggest that one of an ensemble of solution conformations of sLe^x is selected upon binding.

Table 3. Experimental Trans-Glycosidic Scalar Coupling Constants in sLe^x vs Theoretical Values Computed from the 1-ns MD Simulation in Vacuo Using Time-Averaged Restraints

coupling	theoretical	experimental
Neu5Ac C-1−Gal C-3	1.5	nd[a]
Neu5Ac C-3−Gal C-3	2.5	2.1
Neu5Ac C-2−Gal C-2	1.8	1.3
Neu5Ac C-2−Gal C-4	1.1	<1.0
Gal C-2−GlcNAc C-4	3.5	2.9
Gal C-1−GlcNAc C-3	1.6	~2.3
Gal C-1−GlcNAc C-5	0.8	<1.0
Fuc C-2−GlcNAc C-3	2.7	3.3
Fuc C-1−GlcNAc C-2	0.8	<1.0
Fuc C-1−GlcNAc C-4	2.2	2.2
Neu5Ac C-2−Gal H-3	4.6	5.4[b]
Gal H-1−GlcNAc C-4	2.5	2.8[b]
Gal C-1−GlcNAc H-4	5.1	4.8[b]
Fuc H-1−GlcNAc C-3	2.9	2.8[b]
Fuc C-1−GlcNAc H-3	4.2	5.1[b]

[a] Not determined. [b] Experimental values taken from Bizik and Tvaroska.[25]

Bound-State Conformation of the Tetrasaccharide. Typical $F2/F3$ ($^{13}C-^1H$) planes derived from the complex of ^{13}C-sLe^x/E-selectin human IgG chimera (15:1, mole:mole) are shown in Figure 3. As in NOESY/ROESY experiments on the free glycan, much greater spectral dispersion is afforded by the $F2$ (^{13}C) dimension in comparison with 2D NOESY experiments on the complex.[1−3,5] For example, the $F2/F3$ plane at the $F1$ resonance frequency of Fuc H-5 (panel a) shows clearly TRNOEs to both Fuc H-2 and Gal H-6,6′. These TRNOEs have not been observed simultaneously in previous studies.[1−5] In addition, a weak but detectable TRNOE from Fuc H-5 to GlcNAc H-4 is observable in this plane, which has not been observed previously. In total, 11 interresidue TRNOEs could be detected and quantified, and these are listed in Table 4. These data were utilized for the determination of the bound-state conformation of sLe^x by best-fitting the theoretical TRNOE values derived from a full-relaxation matrix simulation to the experimental values by

(24) Poppe, L.; Dabrowski, J.; Vonderlieth, C. W.; Numata, M.; Ogawa, T. *Eur. J. Biochem.* **1989**, *180*, 337−342.

(25) Bizik, F.; Tvaroska, I. *Chem. Zvesti* **1995**, *50*, 84−96.

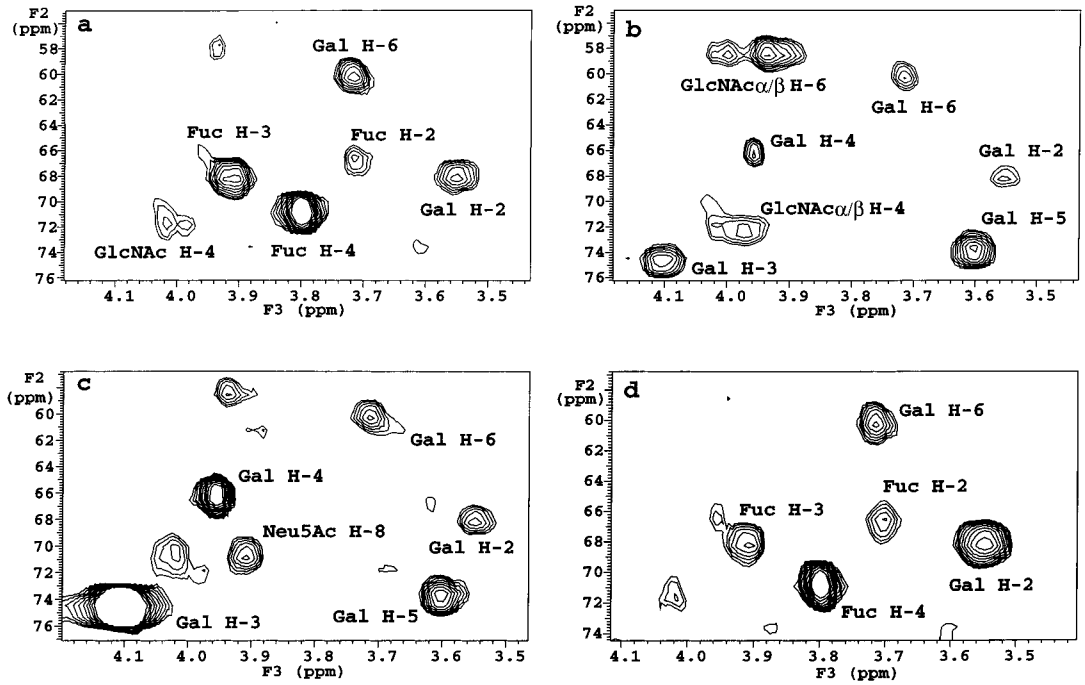

Figure 3. Typical *F*2/*F*3 ($^{13}C/^{1}H$) planes derived from 3D NOESY−HSQC experiment on ^{13}C-enriched sLe^x/E-selectin (15:1 mole/mole). Planes correspond with the *F*1 frequency of (a) Fuc H-5, (b) Gal H-1, (c) Gal H-3, and (d) Fuc CH_3. Authentic transferred NOE cross-peaks in each plane are labeled, and unlabeled cross-peaks correspond with crosstalk from adjacent planes.

Table 4. Experimental TRNOEs Observed in NOESY−HSQC Experiments (τ_m = 150 ms) on sLe^x/E-selectin IgG Chimera (15:1 mole:mole) vs Theoretical Values Computed from Full-Relaxation Matrix Simulations on the Complex

TRNOE connectivity	experimental TRNOE (%)	theoretical TRNOE (%)[a] (a)	(b)	(c)
Fuc H-5−Fuc H-4	6.9	7.1	7.0	7.2
Fuc H-5−Gal H-6	1.5	1.9	5.1	1.3
Fuc H-5−Gal H-2	1.8	1.9	3.6	4.1
Fuc H-5−GlcNAc H-4	0.6	0.5	0.7*	1.3*
Gal H-1−GlcNAc H-6,6′	6.7	11.1	8.3*	15.4
Gal H-1−GlcNAc H-4	4.4	4.9	5.8	5.0
Gal H-3−Neu5Ac H-8	1.0	1.1	3.1	2.4
Fuc CH_3−Gal H-2	4.2	3.6	10.4	12.9*
Fuc CH_3−Gal H-6	1.6	2.1	7.2*	1.9
Fuc H-1−GlcNAc H-3	4.6	5.2	6.2	3.4
GlcNAc CH_3−Fuc H-1	1.6	2.2	3.9	3.0*
GlcNAc CH_3−Fuc H-2	2.4	1.1	1.8*	1.1*

[a] Full-relaxation matrix simulations computed for sLe^x in a conformation which results (a) from best-fitting theoretical TRNOEs to experimental values derived in this study, (b) from the bound-state conformation of sLe^x bound to E-selectin described in ref 4, and (c) from the bound-state conformation of sLe^x bound to E-selectin described in ref 5. The values marked with an asterisk in (b) and (c) indicate TRNOEs that were not actually observed in these respective studies. Parameters used in the simulation are as follow: rotational correlation time of the ligand (τ_{cL}) = 0.24 ns; rotational correlation time of the complex (τ_{cR}) = 110 ns; reduced rate constant (k) = 177 s^{-1}; dissociation constant (K_d) = 0.72 mM;[5] concentration of E-selectin binding sites in the chimera ([R]) = 114 μM; concentration of ^{13}C-sLe^x ([L]) = 1.7 mM; mixing time (τ_m) = 0.15 s.

systematically adjusting the conformation of the glycan using a grid-search procedure. The resulting conformation is shown in Figure 4 and is characterized by the following glycosidic dihedral angles: Neu5Acα2−3Gal, $\phi,\psi = -43°,-12°$; Galβ1−4GlcNAc, $\phi,\psi = +45°,+19°$; Fucα1−3GlcNAc, $\phi,\psi = +29°,+41°$. The values for the Fucα1−3GlcNAc linkage are similar to those determined in the studies of Peters and co-workers,[3,4] which gave rise to glycosidic torsion angles: Neu5Acα2−3Gal, $\phi,\psi = -76°,+6°$; Galβ1−4GlcNAc, $\phi,\psi = +39°,+12°$; Fucα1−3GlcNAc, $\phi,\psi = +38°,+26°$. However, these values differ significantly from those determined in the recent study of Poppe et al.:[5] Neu5Acα2−3Gal, $\phi,\psi = -58°,-22°$; Galβ1−4GlcNAc, $\phi,\psi = +24°,+34°$; Fucα1−3GlcNAc, $\phi,\psi = +71°,+14°$. Conversely, the values for the Neu5Acα2−3Gal linkage agree more closely with the data of Poppe et al.[5] The predicted TRNOE intensities for the derived conformations in each of these studies are included in Table 4. The discrepancy with respect to the Fucα1−3GlcNAc linkage probably derives from the absence of a crucial TRNOE from Fuc CH_3−Gal H-2 in the previous study[5] and from the fact that the interresidue Fuc CH_3−Gal H-6,6′ TRNOE exactly overlaps with the intraresidue TRNOE between Fuc CH_3−Fuc H-2 due to essentially complete overlap of the proton resonances of Gal H-6,6′ and Fuc H-2. This hypothesis is supported by the fact that, under the experimental conditions described in this study, which are very similar to those described in ref 5, the TRNOE from Fuc CH_3−Gal H-2 is predicted to have an intensity of 12.9% in the conformation described in that study (Table 4)

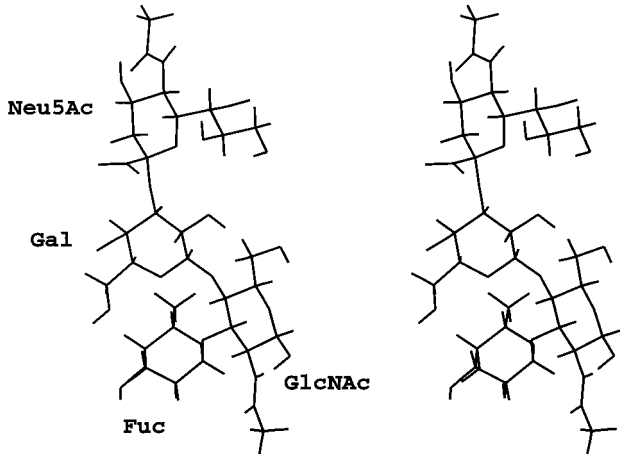

Figure 4. Stereoview of the bound-state conformation of sLe^x derived from transferred NOE measurements.

and should thus have been readily measurable. It is difficult to effect quantitation of these TRNOEs independently to any degree of accuracy using homonuclear ^{1}H NMR methods, whereas in contrast they are well resolved in NOESY−HSQC spectra (Figure 3d).

The discrepancy in the conformation about the Neu5Acα2−3Gal linkage probably derives from the fact that the conformation about this linkage is defined by a single TRNOE between Gal H-3−Neu5Ac H-8 in both this study and previous studies.[1−5] While it can be assumed that the glycan adopts a single conformation in the binding pocket of E-selectin, the discrepancies between the derived values for the glycosidic linkage between studies probably reflects the lack of an adequate number of distance restraints across this glycosidic linkage. Clearly, additional techniques must be developed to obtain additional conformational restraints in systems of this type (Kiddle, G. R., et al., unpublished data). It should also be noted that differences in ^{13}C T_2 relaxation rates as well as differences in $^1J_{H,C}$ coupling constants could, in principle, lead to a distortion of NOE intensities, although the range of values typically encountered in oligosaccharides renders such effects insignificant to first order. A further factor which, in principle, limits the accuracy of the bound-state conformation of sLe^x in all studies to date is the neglect of the influence of protons within the protein binding site. These, by definition, cannot be included in full-relaxation matrix simulations since their relative disposition with respect to the glycan is unknown. While, in principle, the neglect of protein spins from these simulations can lead to erroneous conclusions regarding bound-state conformations,[26,27] the unique associations that are observed in carbohydrate−protein interactions, which involve multiple hydrogen-bond interactions between hydroxyl groups on the glycan and the side chains of binding-site residues in the protein, result in effective magnetic isolation of the carbohydrate ligand from the protein. An exception is the situation where a monosaccharide residue in the glycan partakes in a stacking interaction with an aromatic side chain in the binding site, in which case efficient spin-diffusion is possible involving aromatic side-chain protons due to their proximity to the ligand.[27,28] Fortunately, such stacking interactions can readily be identified as a result of characteristic ring-current shifts of ligand resonances in the presence of the protein.[28] Since no such shifts were observed for the sLe^x/E-selectin complex in the present study, even at low ligand:protein ratios (1:1 mole:mole, data not shown), nor could any ligand−protein TRNOEs be observed at these ratios, these data suggest that the influence of protein spins can be neglected to first order. This conclusion is in accord with saturation-transfer type experiments designed to exclude indirect intraligand TRNOE connectivities via protein protons during the course of transferred NOESY experiments.[5]

The bound-state conformation of sLe^x derived from this study may be compared with the solution conformations described in this study and an earlier study.[22] The conformation about the Neu5Acα2−3Gal linkage ($\phi,\psi = -43°,-12°$) lies closest to minimum "A" and is in a low-energy region of the potential surface,[22,29] but not in the global minimum energy configuation. In contrast, the conformation about the Galβ1−4GlcNAc linkage ($\phi,\psi = +45°,+19°$) appears to be in the global minimum energy configuration for the free tetrasaccharide. The conformation about the Fucα1−3GlcNAc linkage ($\phi,\psi = +29°,+41°$) also lies within the minimum energy region of the potential surface for the free oligosaccharide. With regard to binding affinity, the oligosaccharide, therefore, appears to be bound to E-selectin in a conformation very close to the global minimum energy configuration. The very low affinity of sLe^x for E-selectin, therefore, probably arises from an enthalpy−entropy compensation phenomenon.[30] A possible candidate in this regard is the substantial configurational entropy of the Neu5Ac residue, which must be lost on association at the expense of the free energy of binding as the glycan adopts its "bioactive conformation".

Conclusions

The solution structure and dynamics of sLe^x derived from this study are, in general, similar to those described previously,[22] except that the application of time-averaged distance restraints, made possible by the much larger number of conformational restraints available in the present study, suggests greater conformational freedom about all three glycosidic linkages. In particular, the Fucα1−3Gal linkage accesses a second conformation on the potential surface in addition to the "global minimum" energy conformation defined in the previous study.

The bound-state conformation of sLe^x derived here suggests that the lowest-energy conformation from the repertoire of solution conformations is selected by E-selectin. This conformation differs from that derived from homonuclear ^{1}H NMR methods by Scheffler et al.[3,4] in the orientation of the Neu5Acα2−3Gal linkage, and it also differs from that proposed by Poppe et al.[5] in the conformation about the Fucα1−3GlcNAc linkage. Data obtained in the present study will support current strategies for the design of sLe^x mimics as novel chemotherapeutic agents.[31−34]

Acknowledgment. This work was supported by the Wellcome Trust, Grant Ref. 014973.

JA983423Y

(26) Glaudemans, C. P. J.; Lerner, L.; Daves, G. D.; Kovac, P.; Venable, R.; Bax, A. *Biochemistry* **1990**, *29*, 10906−10911.
(27) Arepalli, S. R.; Glaudemans, C. P. J.; Daves, G. D.; Kovac, P.; Bax, A. *J. Magn. Reson.* **1995**, *B106*, 195−198.
(28) Low, D. G.; Probert, M. A.; Embleton, G.; Seshadri, K.; Field, R. A.; Homans, S. W.; Windust, J.; Davis, P. J. *Glycobiology* **1997**, *7*, 373−381.
(29) Breg, J.; Kroon-Batenburg, L. M. J.; Strecker, G.; Montreuil, J.; Vliegenthart, J. F. G. *Eur. J. Biochem.* **1989**, *178*, 727−739.
(30) Dunitz, J. D. *Chem. Biol.* **1995**, *2*, 709−712.
(31) Jahnke, W.; Kolb, H. C.; Blommers, M. J. J.; Magnani, J. L.; Ernst, B. *Angew. Chem., Int. Ed. Engl.* **1997**, *36*, 2603−2607.
(32) Bänteli, R.; Ernst, B. *Tetrahedron Lett.* **1997**, *38*, 4059−4062.
(33) Kolb, H. C.; Ernst, B. *Chem. Eur. J.* **1997**, *3*, 1571−1578.
(34) Kolb, H. C.; Ernst, B. *Pure Appl. Chem.* **1997**, *69*, 1879−1884.